KLOE Note N.154, February 1996

Evaluation of the performance of the KLOE calorimeter barrel modules at the Cosmic Ray Stand.

C. Bini[b], G. Cabibbo[a ‡], G. Di Cosimo[b], A. Di Domenico[b], P. Gauzzi[b], S. Giovannella[a], S.Han[a,c], S. Miscetti[a]

[a] *Laboratori Nazionali di Frascati dell'INFN Frascati, Italy*
[b] *Università "La Sapienza" e Sezione INFN Roma, Italy*
[c] *IHEP Beijing, China*

1 Introduction

In this note we describe the methods used for the evaluation of the performance of the KLOE calorimeter barrel modules at the Cosmic Ray Test Stand [1] and the results concerning the performance of the first five modules.

This paper is organized in three sections concerning respectively the methods of analysis of the calorimeter pulse height spectra (Sect. 2), of the time spectra (Sect. 3) and the discussion of the five modules performance (Sect. 4).

We use the local KLOE coordinate system [2] and the standard numbering scheme for the 60 elements within a barrel module. The modules are numbered according their construction time at Pol.Hi.Tech. (Modules 0, 3, 6, 8, 12).

The Test Stand uses essentially a streamer tube system (LST in the following) to track cosmic ray particles and evaluate the impact position on the module under test. In the analysis described in this note we used all the events having a single track with an angle (θ) with respect to the vertical of less than $15°$. Furthermore an element is considered having been hit when the Y extrapolated coordinate of the track on the element is in within 0.6 cm of the element borders.

A standard run consists of $4 \div 5$ full-time days of data taking; the statistical accuracy obtained turns out to be sufficient for our purpose (see discussions on each single item). We have done several standard runs for all the tested modules, in such a way as to evaluate also the reproducibility of all the measured variables.

The data structure and the off-line analysis tools (including the LST fitting procedure and the filter) have been described in previous memos [3] [4].

‡Student from Universitá "Tor Vergata" Roma, Italy

2 Analysis of the calorimeter pulse heights.

The pulse height distributions coming from ADC spectra are used to get the attenuation length λ and the collected charge value at $Z = 0$ (the so called MIP which is proportional to the energy deposit of a Minimum Ionizing Particle) for the two sides of each calorimeter element (see Sect. 2.1). Furthermore a special algorithm is used (Sect. 2.2) to determine the average number of photoelectrons $N_{p.e.}$ at $Z = 0$ for each element.

2.1 MIPs and attenuation lengths

In Fig. 1a the scatter plot of ADC vs Z for one of the elements is shown as an example for a standard run. The Z range is divided in 15 slices and for each of them the ADC peak is obtained by fitting the MIP spectrum (see Fig. 2). Fig. 1b shows the dependence of the ADC peak on Z; the superimposed exponential fit gives the attenuation length λ and the MIP. These parameters are obtained with a reproducibility of about 2 % on λ and 0.5 % on MIP.

2.2 Average number of photo-electrons

The distribution of the ratio r_{AB} between the ADC contents of side A and side B for particles impinging at $Z = 0$ does not depend on the Landau fluctuations on the energy deposit since they cancel out in the ratio. The width of such a distribution depends on the fluctuations of the number of photoelectrons $N_{p.e.}$. By means of simple statistical arguments, it can be seen that the root mean square ($R.M.S.$) is related to the average number of photoelectrons as follows:

$$\frac{R.M.S.(r_{AB})}{< r_{AB} >} = \sqrt{\frac{2}{N_{p.e.}}}$$

In Fig. 3 two examples of such distributions are shown and the $N_{p.e.}$ obtained is also indicated. In order to reduce possible bias on the $R.M.S.$, only the events having an ADC value larger than 1/2 MIP in both sides are considered in this analysis.

The method turns out to be reproducible at the level of 10 % but has larger systematical effects (see discussion in Sect. 4). In any case, at the 20 % level it provides average values in agreement with those obtained by the ratio (MIP / Nominal Gain) and is roughly in agreement with what is expected by looking at the time and Z resolutions.

3 Analysis of Time spectra

Due to the large intrinsic time jitter of the trigger (see [1]), only distributions of time differences can be analyzed to get information on the module time resolution. The time resolution (see Sect. 3.1) is obtained by looking at the difference between the TDC values of two consecutive elements (namely two elements belonging to the same row), while the Z resolution (see Sect. 3.2) can be studied directly.

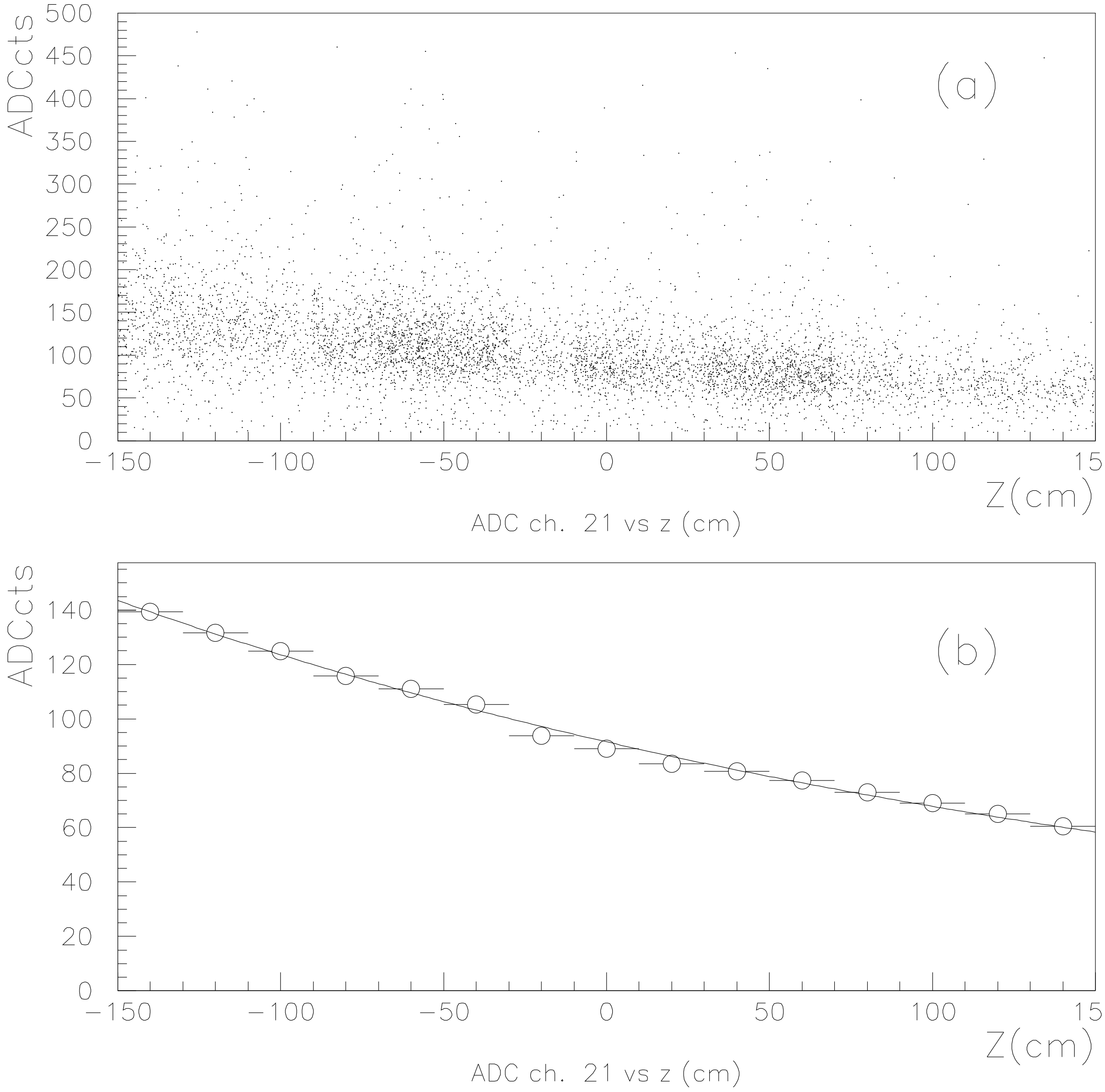

Figure 1: (a) ADC content as a function of the Z-coordinate of the impact position of the particle. (b) ADC peak as a function of Z. The exponential fit is superimposed.

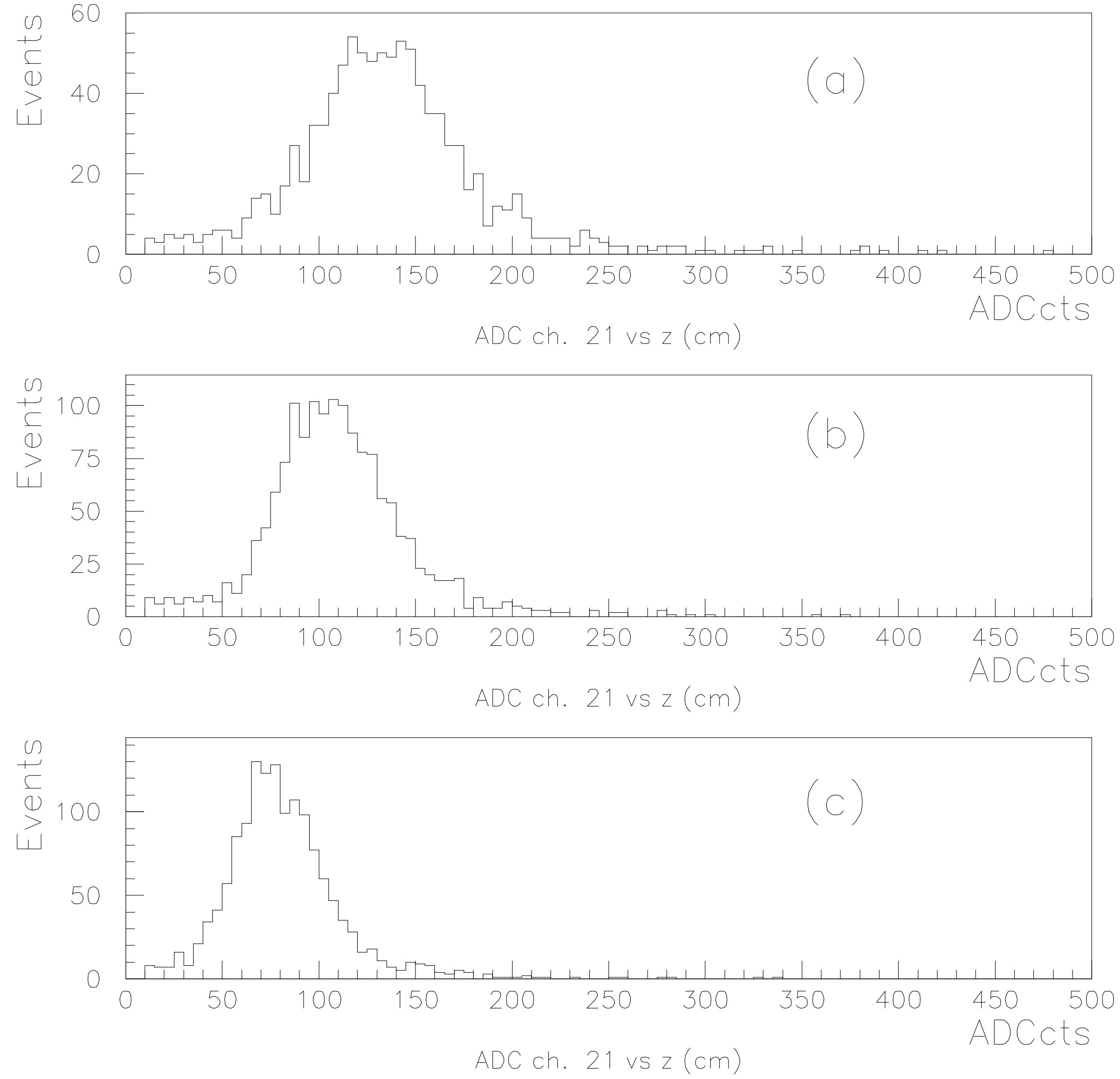

Figure 2: ADC spectra for three slices of the distribution shown in the previous figure. (a) $-130 < Z < -110$ cm, (b) $-50 < Z < -30$ cm and (c) $30 < Z < 50$ cm.

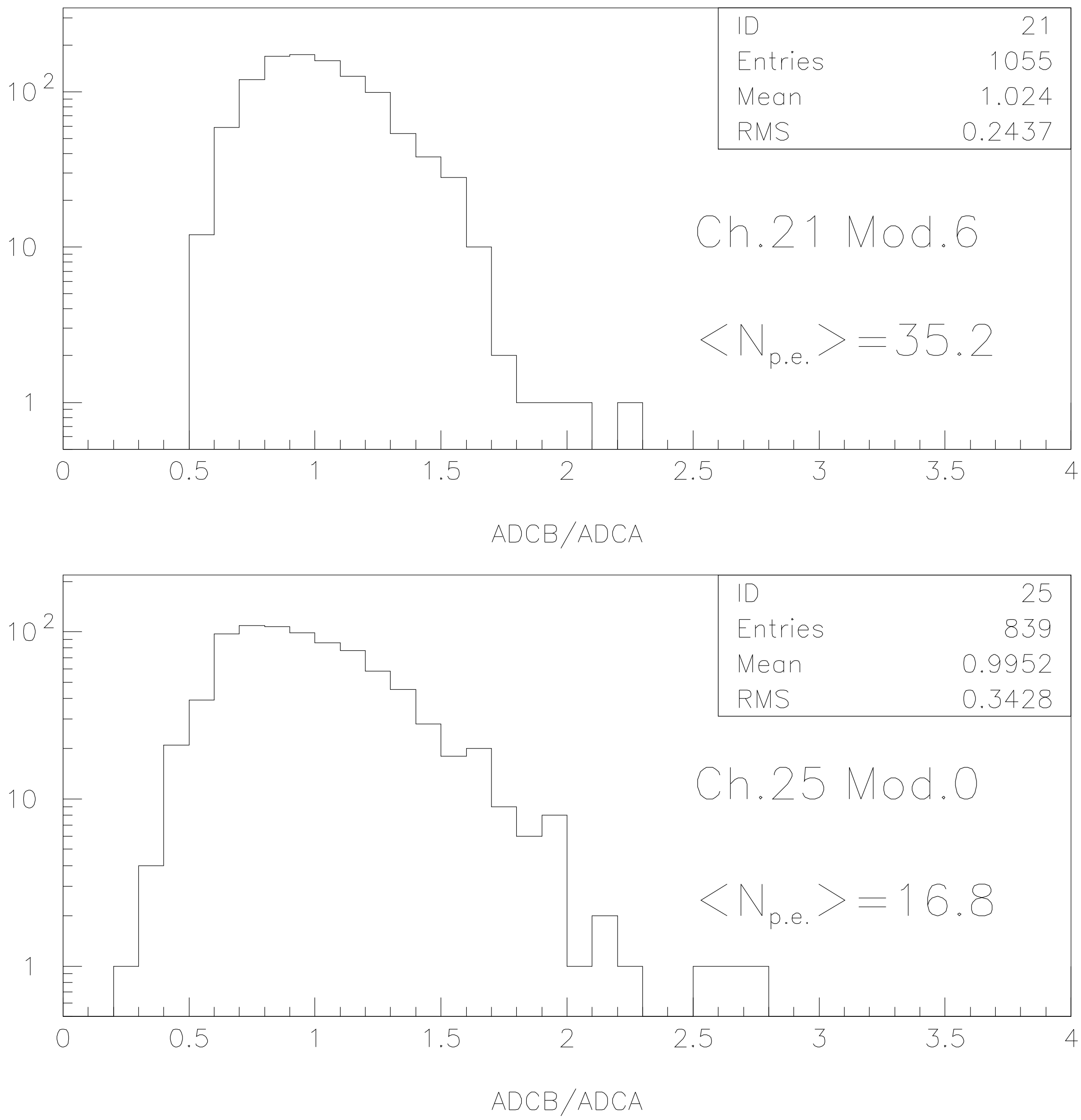

Figure 3: Two examples of the distribution of ratio r_{AB} for a Kuraray element in Mod. 6 (high number of photoelectrons) and for a Pol.Hi.Tech. element in Mod. 0 (low number of photoelectrons).

3.1 Time resolution

Every module consists of 60 elements per side with 12 columns and 5 rows [5]. The first two rows are equipped with Kuraray fibres, the third row is part Kuraray and part Pol.Hi.Tech. and finally the last two rows are equipped with Pol.Hi.Tech. fibres.

We select straight tracks in such a way to make negligible the spread of time of flight between two consecutive elements. Then we take the time differences of the elements belonging to the same column and equipped with fibres of the same type (we assume they have similar time behaviour). So we have 12 couples of Kuraray and 12 couples of Pol.Hi.Tech. elements, i.e. two couples for each column. If i and $i+1$ are the two elements of the couple, we define:

$$\Delta T_A = T_A(i) - T_A(i+1)$$

$$\Delta T_B = T_B(i) - T_B(i+1)$$

$$\Delta T_{sum} = \frac{T(i)_A + T(i)_B}{2} - \frac{T(i+1)_A + T(i+1)_B}{2} = \frac{\Delta T_A + \Delta T_B}{2}$$

In order to get the time resolution σ_t of a single element, we divide the widths of these distributions by $\sqrt{2}$ assuming uncorrelated fluctuations between the two elements concerned.

Since the time resolution scales as $1/\sqrt{N_{p.e.}}$ we expect an exponential behaviour of $\sigma_{\Delta T_A}$ and $\sigma_{\Delta T_B}$ as functions of Z, with slopes that are twice the attenuation lengths λ. Fig. 4 shows examples of $\sigma_{\Delta T_A}$ and $\sigma_{\Delta T_B}$ vs. Z. These curves give attenuation lengths in agreement with those obtained by the ADC analysis (see Sect. 2.1) even if with larger uncertainties.

Fig. 5a shows an example of ΔT_{sum} distribution.

Since the time resolution depends mainly on the calorimeter light yield, a dependence of σ_t on Z $\sigma_t(Z) = \sigma_t(0)\sqrt{\cosh(Z/\lambda)}$ is expected where λ is the attenuation length. As shown in Fig. 5b no relevant dependence is found of σ_t on Z, due to the large value of the attenuation lengths compared to the length of the tested section of the module[‡].

Finally we have verified that the residual time-walk effect (see Fig. 6 where a fit with the usual parametrization T=a+b/$\sqrt{A}$ is also shown) does not affect appreciably the time resolutions (the improvement on σ_t is of the order of 1%) since the effect is only relevant for values of the collected charge much lower than the MIP peak.

3.2 Reconstruction of T_0s and light speed.

The time difference $\Delta T = T_A - T_B$ between the two sides of an element is linearly related to the Z impact position of the particle on the element itself. Fig. 7 shows the dependence of the time-difference on the Z impact position with a linear fit ΔT=a+bZ superimposed. The parameters a and b are related respectively to the $\Delta T^0 = \Delta T(Z=0)$=a and to the light velocity within the fibers v_f=2/b. v_f can be obtained with a 0.2 % uncertainty and ΔT^0 with a 10 ps uncertainty in a standard run.

[‡]The LST system only covers the calorimeter for $-150\,\mathrm{cm} < z < +150\,\mathrm{cm}$.

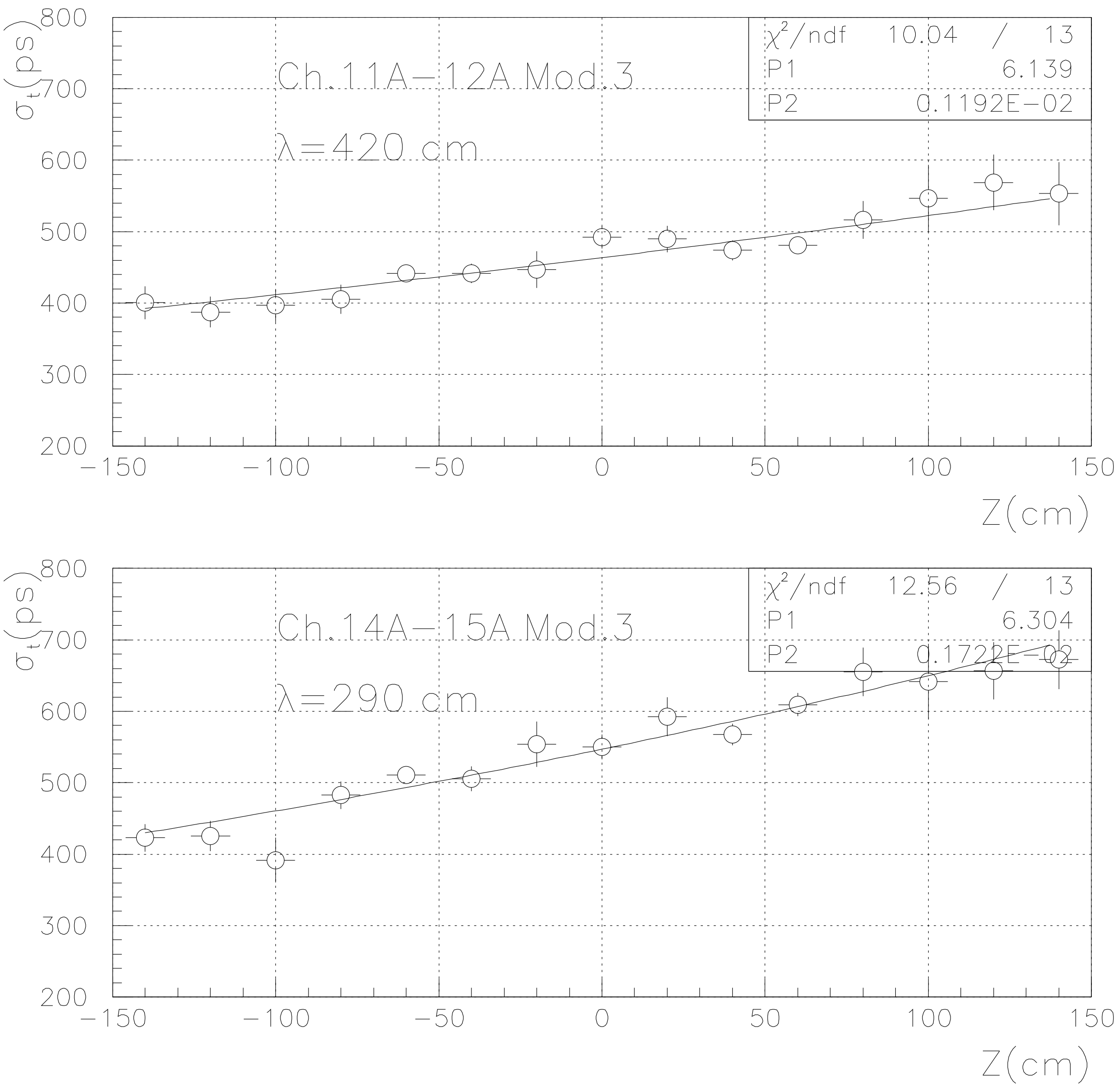

Figure 4: Examples of the dependence of $\sigma_{\Delta T_A}$ on Z for a Kuraray (a) and for a Pol.Hi.Tech. (b) couple of elements.

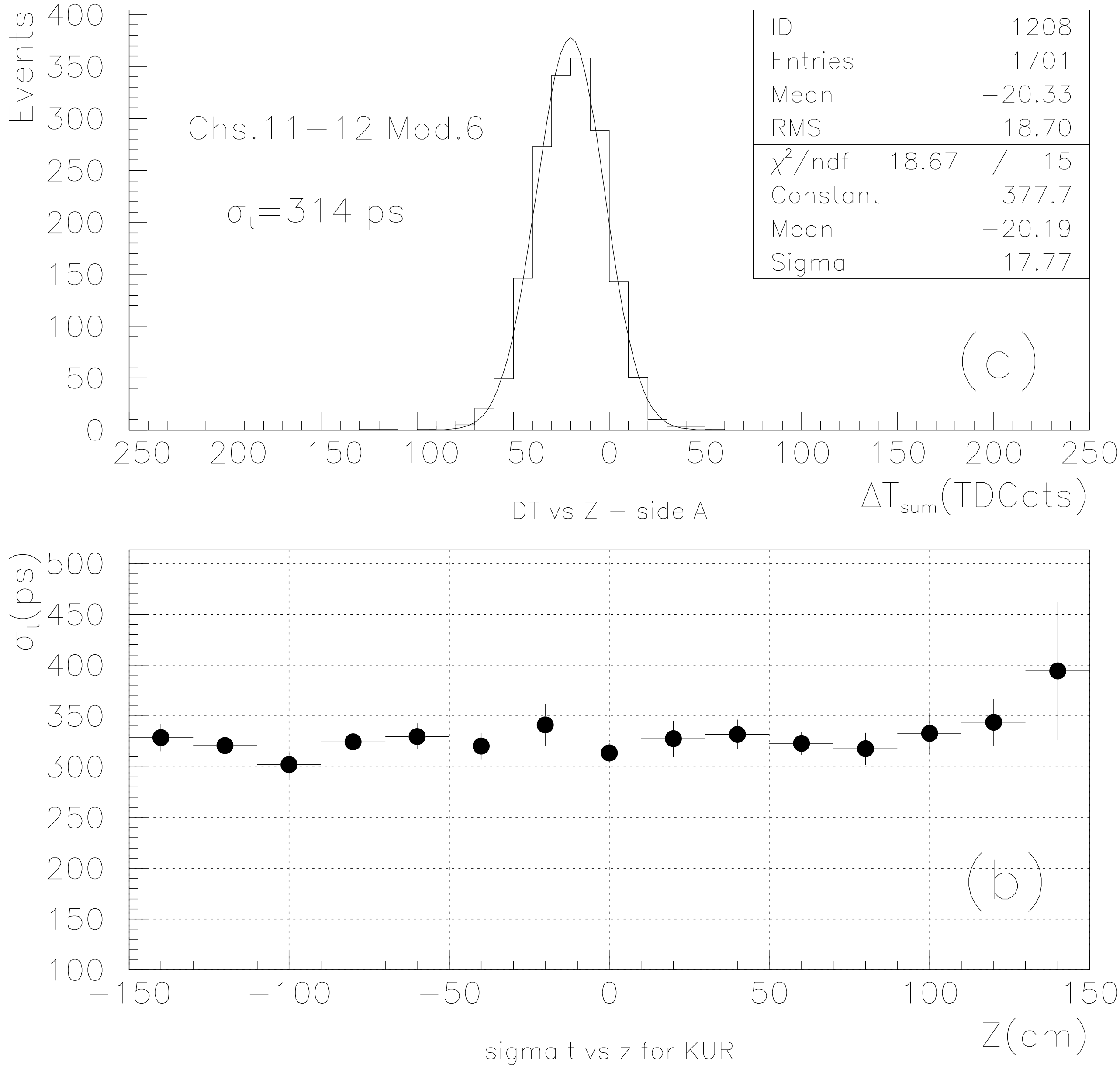

Figure 5: (a) Example of distribution of ΔT_{sum} for a couple of Kuraray elements around $Z = 0$. (b) Dependence of σ_t on Z.

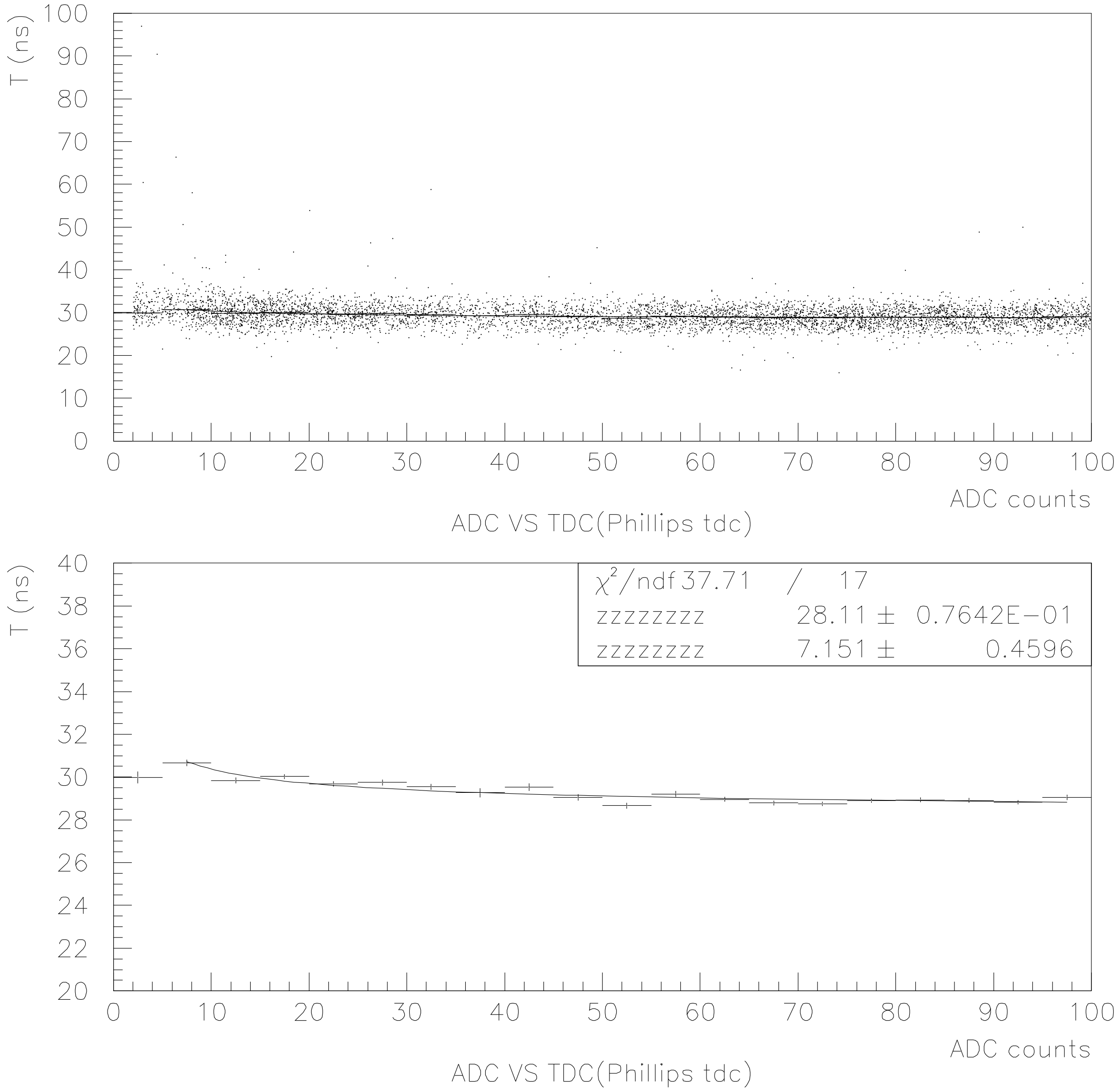

Figure 6: Time vs pulse height plot showing the residual time-walk effect.

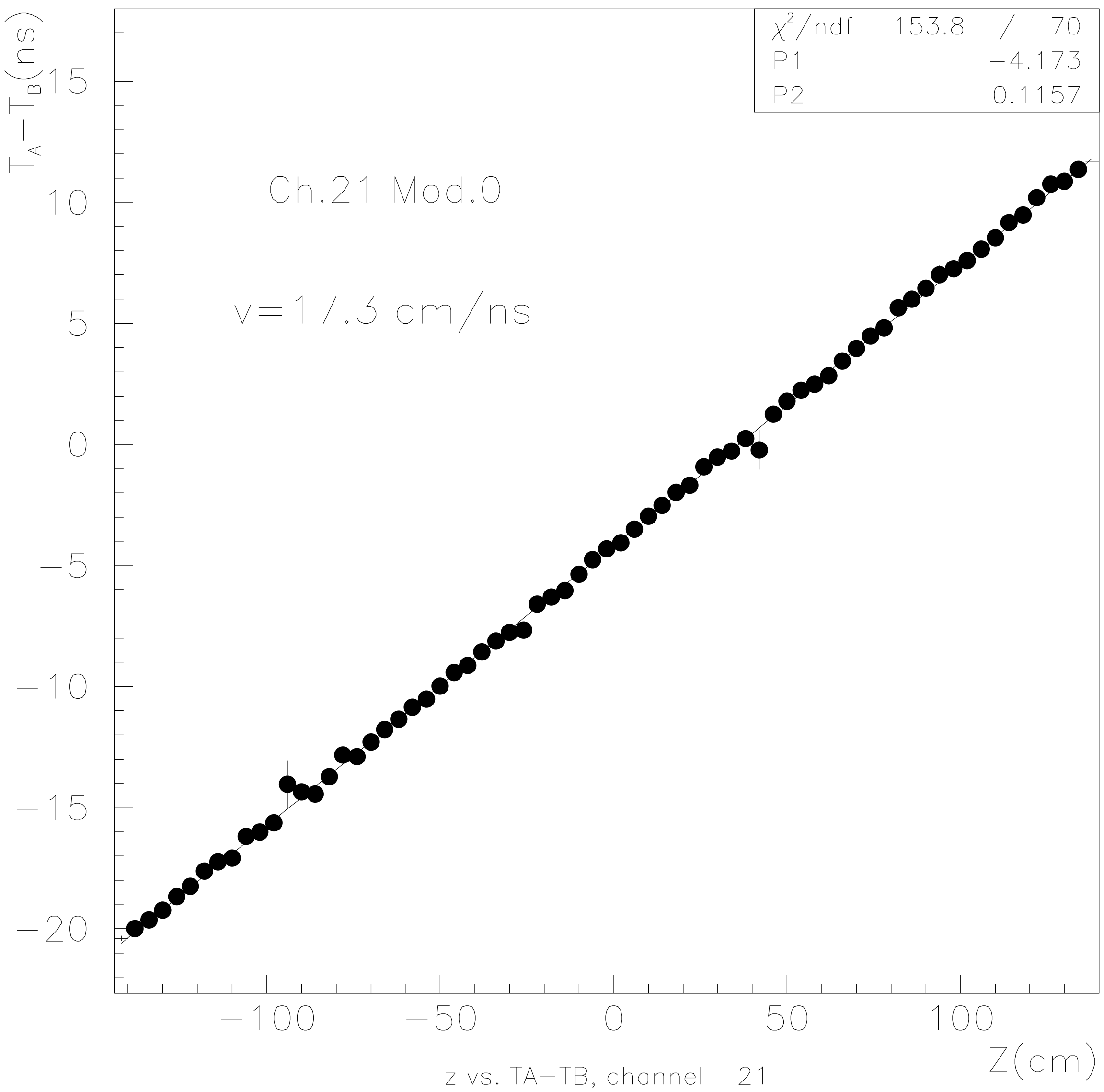

Figure 7: Example of time difference $T_A - T_B$ between the two sides of the same element as a function of the impact coordinate Z of the particle. The value of the light velocity within the fibers is shown.

3.3 Z resolution

The values of ΔT^0 and of v_f are then used to reconstruct (for each calorimeter element) the Z coordinate of the particle as follows: $Z_{rec} = ((T_A - T_B) - \mathrm{a})/\mathrm{b}$. To evaluate the Z resolution σ_Z, the variable $Z_{rec} - Z_{fit}$ is used, where Z_{fit} is the Z extrapolated from the LST fit. In Fig. 8a a typical $Z_{rec} - Z_{fit}$ distribution of a single calorimeter element is shown. If we assume the Z_{fit} resolution negligible (less than 1 cm according to [1]) the σ of the gaussian superimposed is the Z resolution.

As for the case of σ_t and for the same reason, the dependence of σ_Z on Z (see Fig. 8b) is almost flat.

4 Results and discussion

The methods described so far have been applied to Mod. 0 (the first full-size prototype built at Frascati and tested at P.S.I. in summer 1994 [5]) and to the Mod. 3, 6, 8 and 12 all of them built at Pol.Hi.Tech. on October '94 (Mod. 3), February '95 (Mod. 6), March '95 (Mod. 8) and July '95 (Mod. 12) respectively. The measurements were done using photomultipliers Hamamatsu R5946 operated at a nominal gain $\sim 5 \times 10^6$ (including the preamplifier gain) readout through the KLOE front end electronics (splitters, discriminators), Camac ADC and TDC. Two sets of photomultipliers were used. The first set (photomultiplier type 01) has been used from Summer 1994 (during P.S.I. test beam run) up to November 1995 on Mod. 0, 3 and 6. The second set (photomultiplier type 02) from November 1995 on Mod. 6, 8 and 12. The data of Mod. 6 can therefore be used to make a comparison between the two sets of photomultipliers since they are expected to have a different average quantum efficiency.

We give results for 6 configurations: 0/01, 3/01, 6/01, 6/02, 8/02 and 12/02 where the first number identifies the module and the second number indicates the PM set.

The summary of all the results is given in Tab.1. Average values of the parameters described in the previous sections are given separately for elements equipped with Kuraray fibres (Kur.) and for elements equipped with Pol.Hi.Tech. fibres (PHT). σ_t and σ_z are the time and Z resolutions at Z=0.

4.1 Consistency checks

By looking at the table some consistency checks are done.

- The value of the MIP scales roughly as $N_{p.e.}$ for the data with the same set of PM's. This is in agreement with the fact that the PM gain remains constant during the data taking (5×10^6 for the first PM set and a slightly lower value around 4.3×10^6 for the second PM set).
- σ_t and σ_Z scale in such a way that their ratio is constant within few percent.

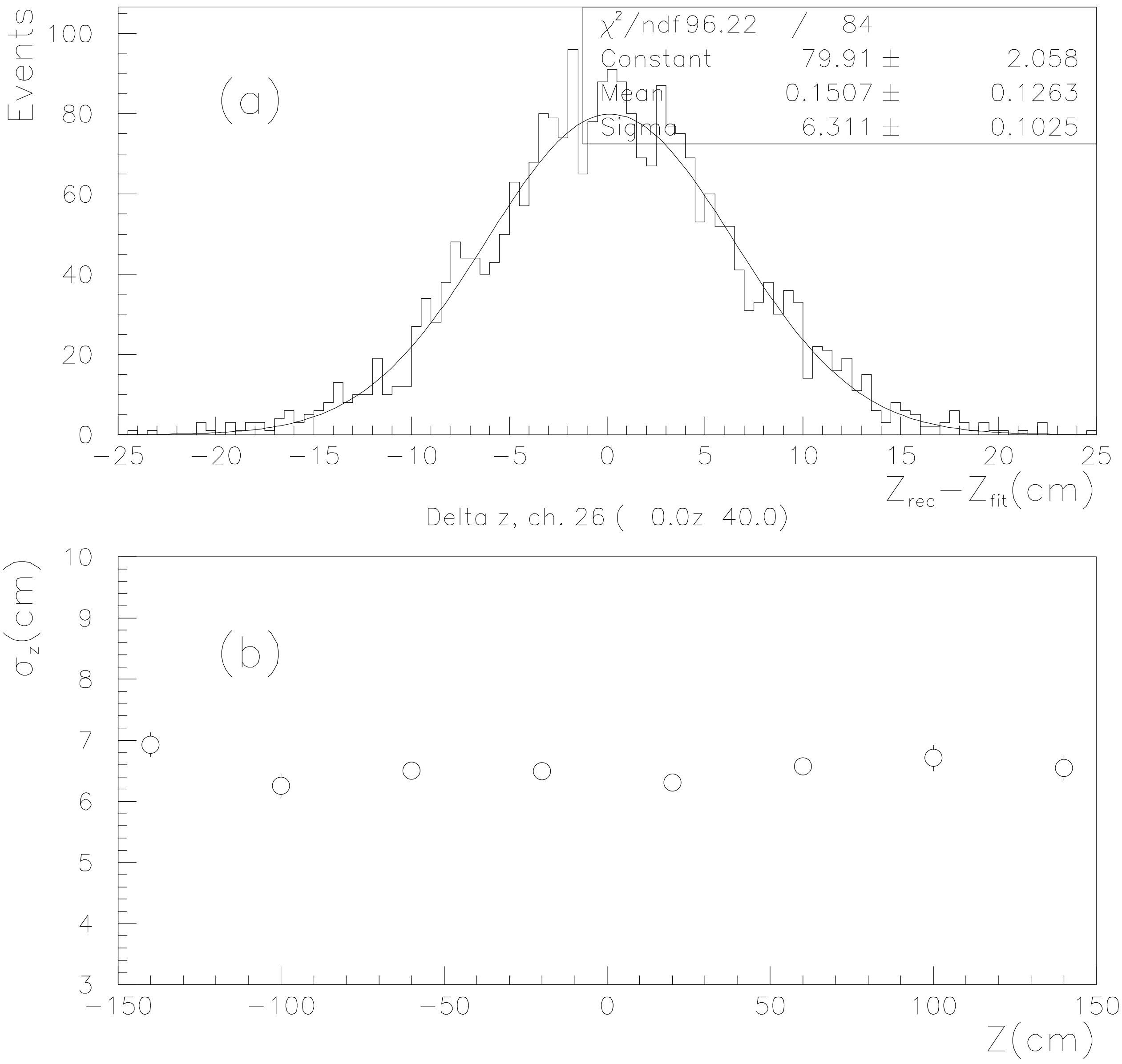

Figure 8: (a) Example of $Z_{rec} - Z_{fit}$ distribution for a single calorimeter element and (b) σ_Z as a function of Z for a Kuraray element in Mod. 0.

Table 1: Summary of the performance of the tested modules.

Parameter	Mod. 0/01	Mod. 3/01	Mod. 6/01	Mod. 6/02	Mod. 8/02	Mod.12/02
λ Kur.(cm)	354 ± 9	430 ± 10	435 ± 9	428 ± 8	431 ± 6	444 ± 6
λ PHT (cm)	234 ± 4	294 ± 5	309 ± 4	306 ± 5	325 ± 5	351 ± 5
MIP (ADC cts) Kur.	78.3 ± 2.9	94.2 ± 3.5	108.3 ± 3.5	95.3 ± 3.1	99.3 ± 5.0	99.1 ± 6.0
MIP (ADC cts) PHT	56.6 ± 1.5	87.4 ± 2.3	102.4 ± 2.9	88.4 ± 1.9	89.8 ± 4.6	95.7 ± 6.0
$N_{p.e.}$ Kur.	24.3 ± 1.3	28.6 ± 0.8	32.0 ± 0.8	35.0 ± 0.7	34.8 ± 1.0	37.6 ± 0.8
$N_{p.e.}$ PHT	18.8 ± 0.5	26.9 ± 0.5	29.9 ± 0.6	31.3 ± 0.6	32.1 ± 0.5	33.3 ± 0.8
$\sigma_t(ps)$ Kur.	385 ± 5	367 ± 11	359 ± 11	313 ± 9	327 ± 12	334 ± 15
$\sigma_t(ps)$ PHT	532 ± 14	423 ± 26	399 ± 11	346 ± 5	321 ± 15	325 ± 7
$\sigma_Z(cm)$ Kur.	6.21 ± 0.10	6.38 ± 0.13	5.88 ± 0.12	5.21 ± 0.08	5.17 ± 0.10	5.37 ± 0.16
$\sigma_Z(cm)$ PHT	8.50 ± 0.16	6.90 ± 0.10	6.39 ± 0.10	5.97 ± 0.18	5.18 ± 0.21	5.03 ± 0.09

- Both σ_t and σ_Z scale only approximately as $1/\sqrt{N_{p.e.}}$. The non perfect scaling for 6/02 8/02 and 12/02 can be due to the intrinsic bias on the method of evaluation of $N_{p.e.}$ that is more significant at higher $N_{p.e.}$.[‡]

From these considerations we conclude that σ_t and σ_z are more reliable than $N_{p.e.}$ as relative estimates of the amount of light.

4.2 Discussion of the results

The results show very clearly an improvement of the quality of the modules from Mod. 0 to Mod. 12.

There is a strong improvement in λ for both kind of fibres going from Mod. 0 to Mod. 3. For the Kuraray the improvement is due to the reduction of the light irradiation damage [6] with the use of yellow filters during the construction. For the Pol.Hi.Tech., it corresponds to the change of the type of fibres. No further improvement in λ from Mod. 3 to Mod. 12 is observed for Kuraray elements while further smaller improvements are observed for the Pol.Hi.Tech. from Mod. 6 to Mod. 12. Furthermore, as expected, λ does not depend on the quality of the photomultipliers.

Concerning the amount of light at the module's center (as shown by $N_{p.e.}$ and by the time and Z resolutions), we observe an overall improvement due to the same reasons quoted

[‡]The method relies on the hypothesis that the width of the ratios distribution is only due to photoelectrons statistics. Any further fluctuations increasing the width, gives a saturation trend to $N_{p.e.}$.

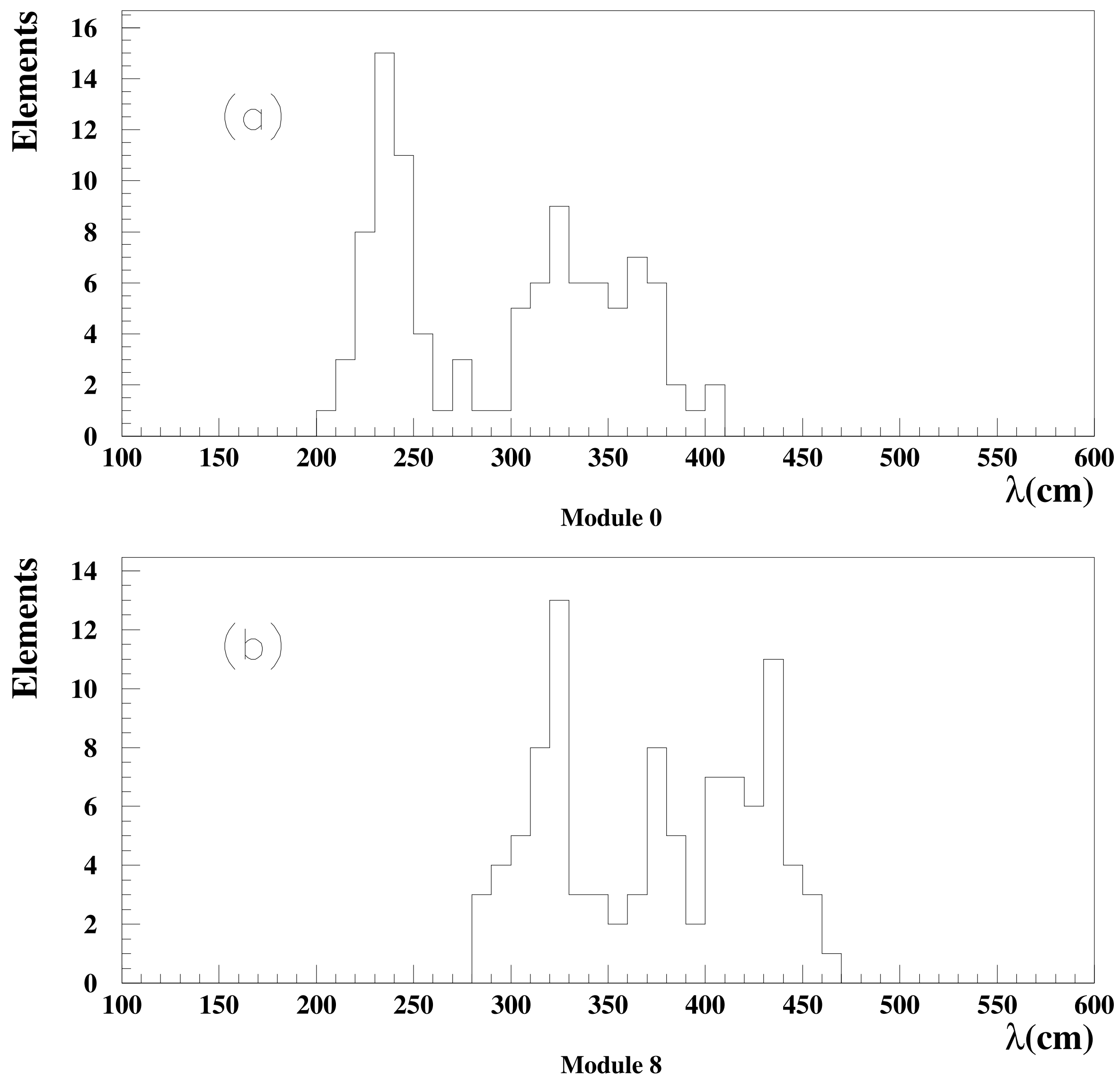

Figure 9: Comparison between the distribution of the attenuation length from Mod. 0 (a) and Mod. 8 (b).

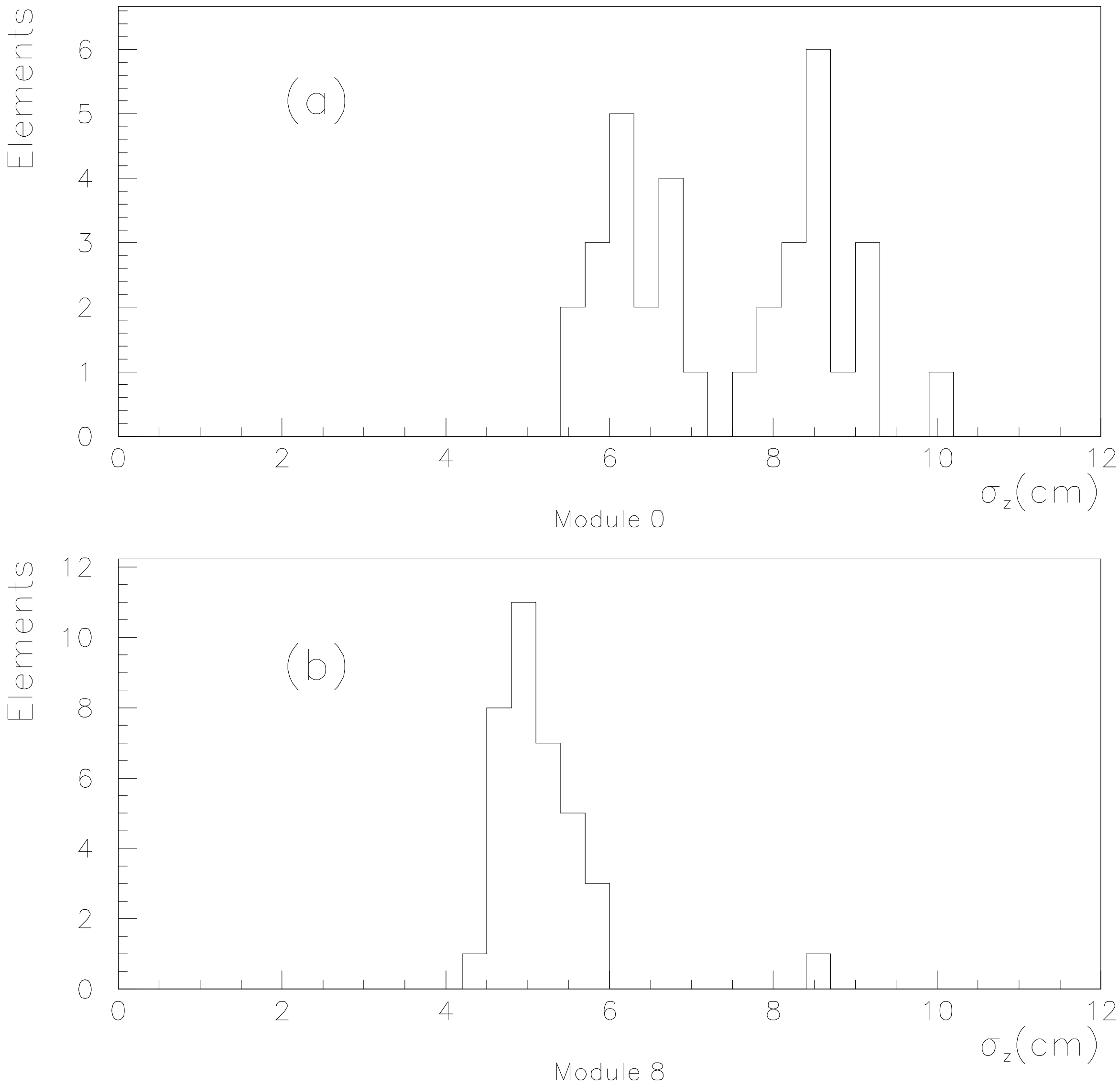

Figure 10: Comparison between the distribution of the σ_z for Mod. 0 (c) and Mod. 8 (d).

above for the effect on λ. Moreover for Mod. 8 and 12 the amount of light at $Z=0$ is the same for the Kuraray and the Pol.Hi.Tech. elements within 10%, so that the response of the different elements is expected to be almost homogenous.

We observe also an improvement improvement with the change of photomultipliers. This improvement is of the order of $8-10\%$ in $N_{p.e.}$ and of $10-12\%$ in terms of both σ_t and σ_Z. These results are not in agreement with the hypothesis of $\sigma_t \sim 1/\sqrt{N_{p.e.}}$ (in that case we would expect an improvement in $N_{p.e.}$ double with respect to the improvement in σ_t and σ_z). As observed at the end of the previous section, this can be explained, since the $N_{p.e.}$ evaluation can be somehow biased; hence the real improvement in $N_{p.e.}$, that is, the improvement in the PM Quantum Efficiency is of the order of $20 \div 24\%$.

Finally we use the time and Z resolution of Mod. 8 and 12 and we scale these numbers assuming that the energy released by a MIP in one element is equal to the amount of energy released by a 32 MeV γ [5]; we find a time and a Z resolution for γ in the experiment of

$$\sigma_t = 58\ ps/\sqrt{E(GeV)}$$

$$\sigma_Z = 0.93\ cm/\sqrt{E(GeV)}$$

This is really a good improvement with respect to the Mod. 0 result of 72 $ps/\sqrt{E(GeV)}$ and 1.24 $cm/\sqrt{E(GeV)}$ respectively[5]. Fig. 9 compares the distributions of λ and fig. 10 of σ_z of Mod. 0 and 8.

5 Conclusions

From the results presented in this note we get the following conclusions:

- there has been a significant improvement in the quality of the fibres with respect to those used in the prototype Mod. 0, due to the increasingly better quality of the Pol.Hi.Tech., and to less light irradiation damage on the Kuraray;
- the new photomultipliers R5946/02 provide an average Quantum Efficiency that is $20 \div 24\%$ higher than that of the R5946/01.

References

[1] M. Anelli et al., KLOE Memo 17, 05/95;

[2] A. Andryakov et al., KLOE Note 115, 09/94;

[3] H. Beker et al., KLOE Memo 24, 06/95;

[4] C. Bini, KLOE Memo 44, 12/95;

[5] S. Woelfle, KLOE Note 134, 01/95;

[6] M. Anelli et al., KLOE Note 136, 01/95;